Nuclear Inst. and Methods in Physics Research, A 1048 (2023) 167995

Contents lists available at ScienceDirect

Nuclear Inst. and Methods in Physics Research, A

journal homepage: www.elsevier.com/locate/nima

A new cylindrical detector for borehole muon radiography

G. Saracino [a,b,*], F. Ambrosino [a,b], A. Anastasio [b], L. Cimmino [a,b], M. D' Errico [b], V. Masone [b], M. Mirra [b], L. Roscilli [b]

[a] *Dipartimento di Fisica, Università degli Studi di Napoli "Federico II', Italy*
[b] *Istituto Nazionale di Fisica Nucleare, sezione di Napoli, Italy*

ARTICLE INFO

Keywords:
Muon radiography
Muography
Borehole detector
Geological prospecting
Geophysics

ABSTRACT

Muons of cosmic origin have a great capability to penetrate through matter. This property is exploited in muon radiography, also known as *muography*, a technique which allows to highlight the presence of discontinuities of the mass density in the subsoil such as cavities, tunnels or rock masses. A detector of cylindrical geometry, optimized for borehole studies and with a diameter of 24 cm, was developed and tested . The scintillation light is read out by 384 Silicon Photomultipliers, directly coupled to the bars. The front-end and acquisition electronics, entirely housed inside the detector, are based on the EASIROC chip and are characterized by limited energy consumption (about 30 W for the entire detector). The detector has been designed in such a way as to simplify its construction as much as possible for its eventual mass production. In this article some details concerning the construction and preliminary results of measurements conducted in the Mt Echia (Naples, Italy) underground are presented.

1. Introduction

Muon radiography has been successfully applied in numerous fields such as archaeology, the study of volcanoes, mining prospecting and the detection of underground cavities. For recent reviews see [1,2]. The principle on which *absorption* muography is based is the measurement of the flux of muons after they have crossed the volume to be inspected. Indeed, the intensity of the flux depends on the average mass density encountered by the muon along its path. By measuring the direction of the muons, a 2D map of the average density as a function of the direction is obtained, which allows to identify anomalies such as cavities or mineral veins. Using measurements acquired from multiple observation points it is possible to obtain 3D information [3].

Some applications require the detector to be placed inside a well. In these cases the optimization of the detector to the cylindrical shape of the hole is fundamental, since, with the same diameter of the well, the greater the sensitive surface and the angular acceptance, the shorter the time required to acquire the necessary data. An interesting borehole detector technology based on scintillator fibers was proposed in [4,5]. This technology, however, requires a number of photon sensors and electronic channels that significantly increases with the size of the diameter (in this specific case 384 electronic channels were used for a 14 cm diameter detector). Furthermore the use of fibers is not simple, requiring attention in their preparation and assembly.

In [6] a borehole detector with scintillator bars and wavelength shifting fiber assembled in a planar geometry is proposed. This kind of geometry simplifies assembly but does not optimize the geometrical acceptance.

A detector which, using arc-shaped plastic scintillators, optimizes angular acceptance and the sensitive surface has been realized and patented. The detector was designed in order to simplify as much as possible the assembling, in the optic to reduce cost for mass production: photon sensors are directly coupled to the scintillators and a special container allows easy positioning of the scintillators.

2. Detector description

In this section the detector is briefly described, for more details see [7,8]. The height and diameter of the detector directly affect its performance, as the number of muons detected per unit of time is directly proportional to the surface area. On the other hand, the dimensions must be compatible with some practical aspects, such as the diameter of the well, the maneuverability inside it, the transportability and the cost. The dimensions of the detector, as regards the sensitive part, are approximately 20 cm in diameter and 1 m in length, while the overall dimensions are 24 cm in height and 130 cm in height

The detector has been designed for applications in urban areas and for depths of the order of 50 m, with an angular resolution allowing the identification of cavities of the order of tens of meters in size at that depths. Regarding the diameter, it was chosen in order to be inserted inside a 25 cm well, which is a diameter that can be realized with

* Corresponding author at: Dipartimento di Fisica, Università degli Studi di Napoli "Federico II', Italy.
E-mail address: giulio.saracino@na.infn.it (G. Saracino).

https://doi.org/10.1016/j.nima.2022.167995
Received 1 July 2022; Received in revised form 16 December 2022; Accepted 18 December 2022
Available online 26 December 2022

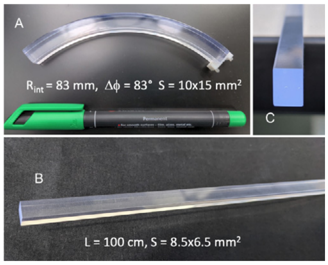

Fig. 1. Example of the plastic scintillators used in the detector. A: An arc-shaped scintillator. B and C: A scintillator bar with rectangular cross section.

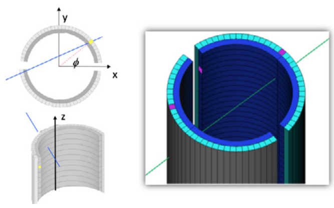

Fig. 2. Example of the determination of the cylindrical coordinates of the impact points of a muon across the detector.

Fig. 3. Left: the detector without the steel cylindrical shell. Right: the detector assembled into the shell.

standard tools, as suggested by our industrial partner TECNO-IN. With respect to the length, it was mainly constrained by the efficiency of the scintillator bars and to the operability of the detector.

The detector is formed by arc-shaped plastic scintillators arranged one above the other horizontally and two lines of plastic scintillator bars, with a rectangular section and arranged vertically to form two half cylinders (see Figs. 1 and 2). Considering the detector positioned with its axis vertically, the impact point of the muon is fully determined by the cylindrical coordinates (ϕ, z) where the ϕ angle is measured by the bars and z by arcs. The average angular resolutions of the muon direction are about 0.7°and 3°in azimuth and zenith respectively.

All the scintillators are inserted in specific containers, produced in *acrylonitrile butadiene styrene* (ABS) by a 3D printer, that define the correct position of the elements and host the front end electronic inside The containers with all the electronic boards are protected by a watertight steel cylinder. The final assembling of the detector is shown in Fig. 3.

Silicon photomultipliers (SiPM) (Hamamatsu S13360-3050PE) with a sensitive area of 3×3 mm^2 are directly coupled to the scintillators.

Front End Electronic (FEE) and Data Acquisition (DAQ) require particular characteristics for this type of application. Compactness is a must, in order to house the electronic boards in the small space inside the cylinder. Low power consumption is also required for at least two reasons. First of all, the detector can operate in places where the electricity grid is not available and therefore it is necessary to resort to alternative sources, such as photovoltaic or wind power. The second

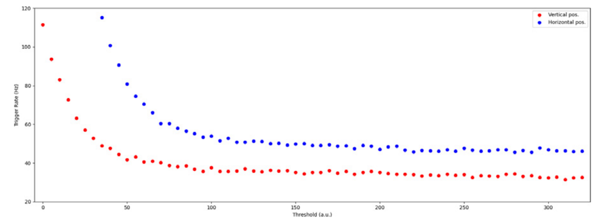

Fig. 4. The trigger rate of the detectors as a function of the discriminator threshold, expressed in arbitrary units of the DAC. The red and blue points correspond to a vertical and horizontal position of the detector, respectively. See the text for more details.

reason is that the detector is protected by a watertight steel cylinder. The heat exchange with the outside is therefore limited and excessive energy consumption would lead to unacceptable overheating inside the detector.

The FEE and DAQ was developed on the experience maturated in previous muon radiography projects [9,10]. The FEE is based on the *EASIROC* ASIC specific for SiPM readout and characterized by low power consumption and compactness. The detector has, in total, 384 Silicon photomultipliers. Each EASIROC can read 32 SiPMs and a total of 12 boards are used for the detector. Each board produces a fast logic signal (OR32) if at least one of the 32 SiPM signals exceeds a programmable voltage threshold produced by a Digital to Analogical Converter (DAC). The FEE boards are controlled by a *MASTER* board based on a FPGA for the data transfer with the FEE and a *RaspberryPi-2* computer for the control of the DAQ and internet communication. The MASTER receives all the 12 OR32 logical signals from the FEE boards and produces a trigger logic signal according to a programmable trigger logic in order to start data acquisition from all FEE boards. The total power consumption, including the *RaspberryPi* and the *Arduino-UNO* controller for the temperature and humidity measurements inside the detector, is about 30 W. At start-up, the detector temperature increases, with respect to the environmental one, due to the power dissipation of the electronic hosted inside the detector, reaching a stable value that depends mainly on the environmental temperature. As an example, for an environmental temperature of 20 °C. The temperature measured inside the detector cylinder was around 35 °C. The SiPM bias voltage was set in order to maintain the same photo-detection efficiency at 20 °C. No degradation in the detector performance was observed.

3. Measurements results

During the detector commissioning the muon rates in *open sky* mode was measured. The detector was positioned at the ground surface with no object between the detector and the sky, with the exception of the roof of the container where the detector was positioned. The measurements confirmed the good performances of the detector, as shown below. The trigger rate of the detector as a function of the discriminator thresholds (see Section 2) is shown in Fig. 4. A common value for the 12 thresholds of the discriminators is changed. The trigger logic selects events where a muon crosses at least one of the two semicylinder. In the plot it is possible to observe a region of low threshold values where accidental coincidences, due to SiPMs dark counts, are dominant. For higher threshold values (corresponding at about more than 5 photoelectrons), the detector shows a large *plateau* where the rate of detected muons is stable. Figs. 5 and 6 show the good agreement between the measured and the expected muon rates in open-sky. The expected flux was computed with the Gaisserś modified model [11] and a simplified detector model that takes in account only the geometrical efficiency of the detector, including dead spaces.

Successively a measurement campaign in the underground of Mt Echia was performed. Mt Echia is an ancient and complex system of galleries and cavities, where known cavities were previously measured

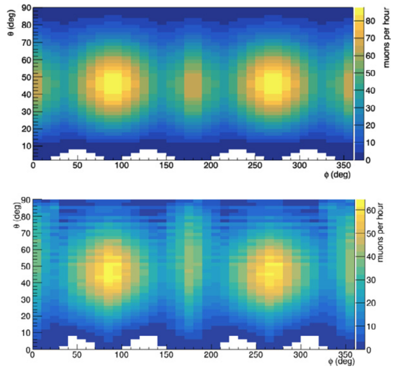

Fig. 5. Comparison between expected (top figure) and measured (bottom) muon rates as a function of the elevation and azimuth angles.

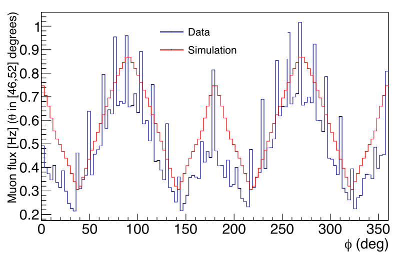

Fig. 6. Comparison between expected (top figure) and measured (bottom) muon rates as a function of the azimuth angles at the zenith angle of about 46.5°.

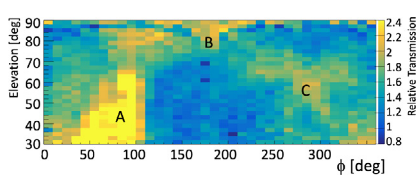

Fig. 7. Example of a muon radiography obtained in the Mt Echia underground. The Relative Transmission is plotted as a function of the elevation and azimuthal angles. Regions labeled with the letters A, B and C correspond to angular regions where known cavities are present and are characterized by values of R greater than 1.

wit a planar detector of 1 m^2 of sensitive area [3,12]. In order to identify the presence of cavities, the relative transmission $R(\alpha,\phi)$ is used, defined as the ratio, for each direction (α,ϕ), between the measured transmission and the transmission obtained from simulations where no cavities are included. The measured transmission is obtained by the ratio between the muons rates measured in the underground and the one observed in *open sky*.

As an example Fig. 7 shows the relative transmission obtained placing the detector in a position where known voids, with a volume of the order of one hundred of m^3 and distances from the detector in the range between 5 to 30 m, are in the angular acceptance of the detector. Values of $R(\alpha,\phi) \sim 1$ correspond to directions where the measurement values and model ones are in agreement, i.e. no cavities are crossed by muons. Instead values of $R(\alpha,\phi) > 1$ correspond to an excess of muons with respect to the model, i.e. a cavity is present in that direction. All the known cavities are well identified and the results are in agreement with the results obtained with the planar detector, confirming the capability of the cylindrical detector to detect voids (for more details see [7,8]).

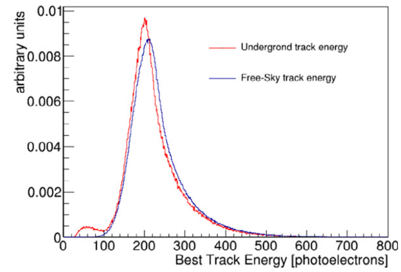

Fig. 8. Total energy distribution, expressed in number of photoelectrons, of the reconstructed track. This is obtained as the sum of all clusters energies involved in the track. Blu line:open sky sample. Red: underground sample. See the text for more details.

During the measurements an anomalous trigger rate, with respect to the expected muon flux was observed ($\sim$ 100 Hz instead of $\sim$ 1 Hz with a trigger logic that requires at least two energy clusters produced simultaneously). This phenomenon has been attributed to environmental radioactivity. The hill of Mt Echia is of yellow tuff of volcanic origin. As reported for example in [13], this rock contains many radioactive isotopes as ^{232}Th ^{226}Ra and ^{40}K. Since the detector is protected by a 3 mm thick steel tube, watertight, the observed signals are not attributed to α or β emissions but to γ. For instance ^{232}Th daughters ^{212}Bi, ^{208}Tl and ^{228}Ac produce γ of 727, 860 and 911 keV respectively, and can trigger the detector. Most of these events are not able to produce a track (that requires at least four energy clusters) and are rejected during the analysis. Anyway a small amount of tracks presents a total energy deposition that is not compatible with the one observed with *opensky* sample (see Fig. 8). These tracks have been attributed to the radioactivity background and have been discarded applying an energy cut. The small difference between the distributions of the energies deposited by muons is probably due to the different angular distribution of the muons in the underground and in free-sky, since the cluster energy depends on the angle of impact of the muon with the scintillators.

4. Conclusions

A new type of borehole detector, based on plastic scintillator elements and with a cylindrical geometry, was realized and tested for muography applications. This specific geometry optimizes the sensitive area and the angular acceptance of the detector. The detector has an average angular resolutions of about 0.7°and 3°in azimuth and zenith respectively and a geometrical acceptance of 360°in azimuth and between 15°and 90°in zenith, in vertical position. Tests conducted in *open sky* have shown a good agreement with the expected muon rates and stable detector's performances. Excellent results were obtained during a measurement campaign in the underground of a tuff hill in Naples (IT), where known cavities have been detected in few days of data acquisition. A small amount of events due to natural radioactivity background was observed and rejected in data analysis.

Declaration of competing interest

The authors declare that they have no known competing financial interests or personal relationships that could have appeared to influence the work reported in this paper.

Acknowledgments

The realization of the detector prototype was supported by the *STRESS* S.C.a R.L. company, in the frame of the project *METROPOLIS* - PON 03PE 00093 4 and TECNO-IN S.P.A. The authors gratefully acknowledge the *Associazione Culturale Borbonica Sotterranea* for the measurements in Mt Echia.

References

[1] G. Bonomi, P. Checchia, M. D'Errico, D. Pagano, G. Saracino, Applications of cosmic-ray Muons, Prog. Part. Nucl. Phys. 112 (2020) 103768, http://dx.doi.org/10.1016/j.ppnp.2020.103768.

[2] L. Olah, H.K.M. Tanaka, D. Varga editors, Muography Exploring Earth's Subsurface with Elementary Particles, in: American Geophysical Union Geophysical Monograph Series 2022, Vol. Online ISBN:9781119722748, 2022, http://dx.doi.org/10.1002/9781119722748.

[3] L. Cimmino, et al., 3D muography for the search of hidden cavities, Sci. Rep. 9 (2019) 2974, http://dx.doi.org/10.1038/s41598-019-39682-5.

[4] M. Menichelli, S. Ansoldi, M. Bari, M. Basset, R. Battiston, S. Blasko, F. Coren, E. Fiori, G. Giannini, D. Iugovaz, A. Papi, S. Reia, G. Scian, A scintillating fibres tracker detector for archaeological applications, Nucl. Instrum. Methods Phys. Res. A 572 (1) (2007) 262–265, http://dx.doi.org/10.1016/j.nima.2006.10.317, Frontier Detectors for Frontier Physics.

[5] M. Basset, S. Ansoldi, M. Bari, R. Battiston, S. Blasko, F. Coren, E. Fiori, G. Giannini, D. Iugovaz, M. Menichelli, S. Reia, G. Scian, MGR: An innovative, low-cost and compact cosmic-ray detector, Nucl. Instrum. Methods Phys. Res. A 567 (1) (2006) 298–301, http://dx.doi.org/10.1016/j.nima.2006.05.099, Proceedings of the 4th International Conference on New Developments in Photodetection.

[6] A. Bonneville and R et al, J. Kouzes, C. Yamaoka, E. Rowe, J. Guardincerri, C. Durham, D. Morris, K. Poulson, D. Plaud-Ramos, J. Morley, J. Bacon, J. Bynes, C. Cercillieux, K. Ketter, I. Le, G. Mostafanezhad, J. Varner, A. Flygare, A. Lintereur, A novel Muon detector for borehole density tomography, Nucl. Instrum. Methods Phys. Res. A 851 (2017) 108–117, http://dx.doi.org/10.1016/j.nima.2017.01.023.

[7] L. Cimmino, F. Ambrosino, A. Anastasio, M. D'errico, V. Masone, L. Roscilli, G. Saracino, A new cylindrical borehole detector for radiographic imaging with muons, Sci. Rep. 2021 11 (2021) http://dx.doi.org/10.1038/s41598-021-96247-1, 17425.

[8] L. Cimmino, F. Ambrosino, A. Anastasio, M. D'errico, V. Masone, L. Roscilli, G. Saracino, A Borehole muon telescope for underground Muography, J. Adv. Instrum. Sci. (2022) http://dx.doi.org/10.31526/Jais.2022.279.

[9] F. Ambrosino, et al., The MU-RAY project: Detector technology and first data from Mt. Vesuvius, J. Instrum. 9 (02) (2014) http://dx.doi.org/10.1088/1748-0221/9/02/c02029.

[10] L. Cimmino, et al., The MURAVES telescope front-end electronics and data acquisition, Ann. Geophys. 60 (1) (2017) http://dx.doi.org/10.4401/ag-7379.

[11] M. Guan, M.-C. Chu, J. Cao, K.-B. Luk, C. Yang, A parametrization of the cosmic-ray Muon flux at sea-level, URL https://arxiv.org/abs/1509.06176v1.

[12] G. Saracino, et al., Imaging of underground cavities with cosmic-ray muons from observations at Mt. Echia (Naples), Sci. Rep. 7 (2017) 1038, http://dx.doi.org/10.1038/s41598-017-01277-3.

[13] V. Roca, C. Sabbarese, A. D'Onofrio, A. Ermice, I. Inglima, C. Lubritto, M. Pugliese, F. Terrasi, G. Migliore, Natural radioactivity of building materials coming from a volcanic region, 2004.